Different Levels of the Homeodomain Protein Cut Regulate Distinct Dendrite Branching Patterns of *Drosophila* Multidendritic Neurons

Wesley B. Grueber, Lily Y. Jan, and Yuh Nung Jan*
Howard Hughes Medical Institute
Department of Physiology
Department of Biochemistry
University of California, San Francisco
533 Parnassus Avenue, Room U226
San Francisco, California 94143

Summary

Functionally similar neurons can share common dendrite morphology, but how different neurons are directed into similar forms is not understood. Here, we show in embryonic and larval development that the level of Cut immunoreactivity in individual dendritic arborization (da) sensory neurons correlates with distinct patterns of terminal dendrites: high Cut in neurons with extensive unbranched terminal protrusions (dendritic spikes), medium levels in neurons with expansive and complex arbors, and low or nondetectable Cut in neurons with simple dendrites. Loss of Cut reduced dendrite growth and class-specific terminal branching, whereas overexpression of Cut or a mammalian homolog in lower-level neurons resulted in transformations toward the branch morphology of high-Cut neurons. Thus, different levels of a homeoprotein can regulate distinct patterns of dendrite branching.

Introduction

The vast diversity of neuronal morphology underlies the varied ways that individual neurons receive and transmit sensory and presynaptic inputs (Häusser et al., 2000; Jan and Jan, 2001; Scott and Luo, 2001; Vetter et al., 2001). Neurons of similar functions often exhibit common features of dendritic arborization, allowing their classification based on morphological criteria (Ramon y Cajal, 1911; Wässle and Boycott, 1991; MacNeil and Masland, 1998). How different classes of neurons acquire their distinct dendritic patterns likely involves both intrinsic and extrinsic control of branching, growth, and stabilization (Koester and O'Leary, 1992; Threadgill et al., 1997). The identities of factors that endow neurons with their characteristic dendritic arbors are, however, largely unknown.

Drosophila dendritic arborization (da) sensory neurons, named for their multiple branched dendrites that innervate the larval epidermis, provide an excellent system for exploring the basis of class-specific dendritogenesis. As with other *Drosophila* peripheral sensory neurons, da neurons are born early during embryonic development (Bodmer et al., 1989) and acquire their proper identities by the activity of proneural genes coding for basic helix-loop-helix (bHLH) proteins and downstream identity selector genes including *cut* (Dambly-

Chaudière and Ghysen, 1987; Blochlinger et al., 1988; Jarman et al., 1993; Brewster and Bodmer, 1995; Brewster et al., 2001). Despite an apparently common requirement for these early acting genes, each of the 15 abdominal da neurons per hemisegment acquires one of four types of dendritic arbor morphologies (Grueber et al., 2002). These classes (termed classes I–IV) show pronounced morphological differences, such as progressively larger dendritic fields and more extensive branching patterns. However, class III neurons have one additional feature, namely, numerous short terminal branches extending from their main dendritic trunks (here we call these structures "dendritic spikes"). Are these divergent dendrite morphologies specified by different intrinsic factors? What might such factors be? Are they distinct from the proneural and identity selector genes?

In pursuing these questions, we examined the role of *cut* because of its expression pattern and function in the peripheral nervous system (PNS). *cut* is expressed in both external sensory (es) organs and at different levels among the da neurons (Blochlinger et al., 1990). Loss of Cut activity from es organs causes a morphologic and antigenic switch to a chordotonal (ch) organ identity (Bodmer et al., 1987) and antigenic changes in da neurons (Brewster and Bodmer, 1995; Brewster et al., 2001). Chordotonal and es neurons both have single, unbranched dendrites, but these dendrites differ in their fine morphology (Merritt, 1997). The role of Cut in da neuron morphogenesis, by contrast, is not known. We wondered whether da neurons showing high, medium, or undetectable levels of Cut (Blochlinger et al., 1990) correspond to different classes of neurons with distinctive types of dendritic arbors (Grueber et al., 2002). If such a correlation exists, it would bring us to the next question: do different levels of Cut contribute to morphological distinctions between da neuron dendrites?

Here, we report that da neurons showing different levels of Cut immunoreactivity, along with those that do not show detectable Cut expression, correlate with independently derived morphological classes. Neurons belonging to a class characterized by short dendritic spikes showed uniformly stronger labeling than did neurons with other types of dendritic morphologies. Loss of *cut* function due to mitotic recombination caused morphological defects in all classes that express this gene and, in particular, caused a loss of spikes from the high-expressing neurons. Conversely, Cut overexpression in neurons that show relatively lower levels of immunoreactivity caused extensive dendrite branching and growth of terminal dendritic spikes. These data suggest that the level of Cut expressed by different da sensory neurons regulates class-specific dendrite morphogenesis.

Results

Organization of the *Drosophila* Dendritic Arborization System

Drosophila sensory neurons can be divided into three major types: external sensory (es), chordotonal (ch)

*Correspondence: ynjan@itsa.ucsf.edu
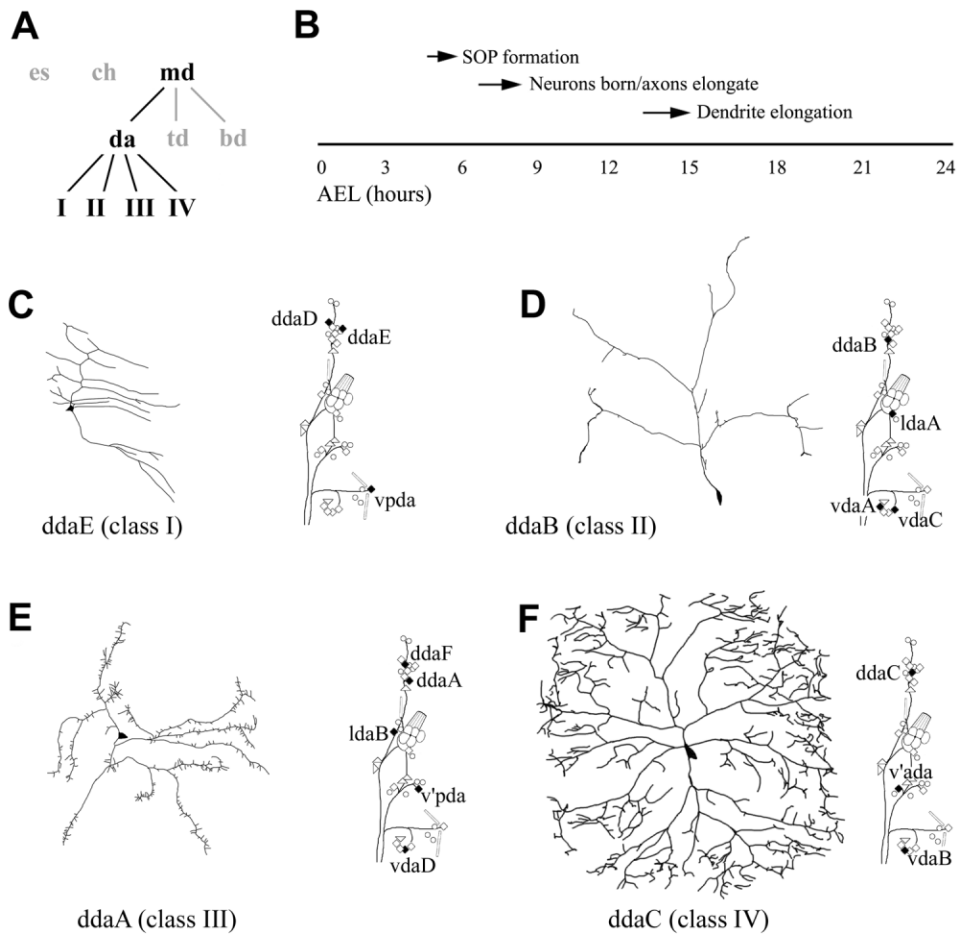
Figure 1. Development of Different Morphological Classes of da Neurons

(A) The different classes of trunk sensory neurons in *Drosophila*. Neurons that are the focus of this study are shown in black.

(B) Timeline of the embryonic development of da neurons.

(C–F) Mature morphologies of representative class I (C), class II (D), class III (E), and class IV (F) da neurons with the positions of other same-class neurons (closed diamonds) in a schematized abdominal hemisegment of the PNS. Note that the typical positions of vdaD and ddaF are shifted slightly ventral from what was previously reported (Grueber et al., 2002). Dorsal is up and anterior is to the left in all panels.

(both with single dendrites), and multidendritic (md) neurons (Bodmer and Jan, 1987). The md neurons are further subdivided into the dendritic arborization (da) neurons, the tracheal dendrite (td) neurons, and the bipolar dendrite (bd) neurons (Figure 1A; Bodmer and Jan, 1987). The da neurons differ from these other types by having extensively branched dendrites that innervate the epidermis. All da neurons are born by 9 hrs after egg laying (AEL) (Figure 1B) (Bodmer et al., 1989) and soon thereafter begin to project axons toward the ventral nerve cord. Peripheral dendritogenesis is initiated several hours later, at around 13 hr AEL (Figure 1B) (Gao et al., 1999). The extension and branching of these nascent dendrites can be followed in living embryos using the Gal4-UAS binary expression system (Brand and Perrimon, 1993) to express GFP (and variants such as mCD8::GFP) in all or specific subsets of da neurons. In this study, we have used either *elav-Gal4* or $Gal4^{109(2)80}$ (Gao et al., 1999) to label all da neurons, and $Gal4^{221}$ and $Gal4^{477}$, which were identified in an enhancer trap screen (D. Cox, G. Tavosanis, W.G., B. Ye, U. Heberlein, unpublished data) to

label subsets of da neurons beginning late in embryogenesis.

A characterization of the peripheral dendrite morphologies of larval da neurons using the MARCM system (for mosaic analysis with a repressible cell marker) prompted a segregation of the 15 neurons in each abdominal hemisegment into four morphological classes (classes I–IV; Figures 1C–1F) (Grueber et al., 2002). To characterize the proneural gene requirements of these neurons, we introduced the sc^{B57} deficiency into a $Gal4^{109(2)80}$ background. Loss of proneural genes in the *achaete-scute* complex (*ASC*) eliminated class II, III, and IV da neurons, and at least one of the dorsal class I da neurons (likely ddaD; data not shown). As shown previously, the *atonal*-dependent vpda neuron was unaffected (Jarman et al., 1993). Remaining in the dorsal cluster were the *amos*-dependent dorsal bipolar dendrite neuron (Huang et al., 2000), an as yet unidentified dorsal neuron, and an *amos*-dependent dorsal neuron (Brewster et al., 2001; henceforth referred to as dmd1) that sends its dendrites to an internal nerve (likely the
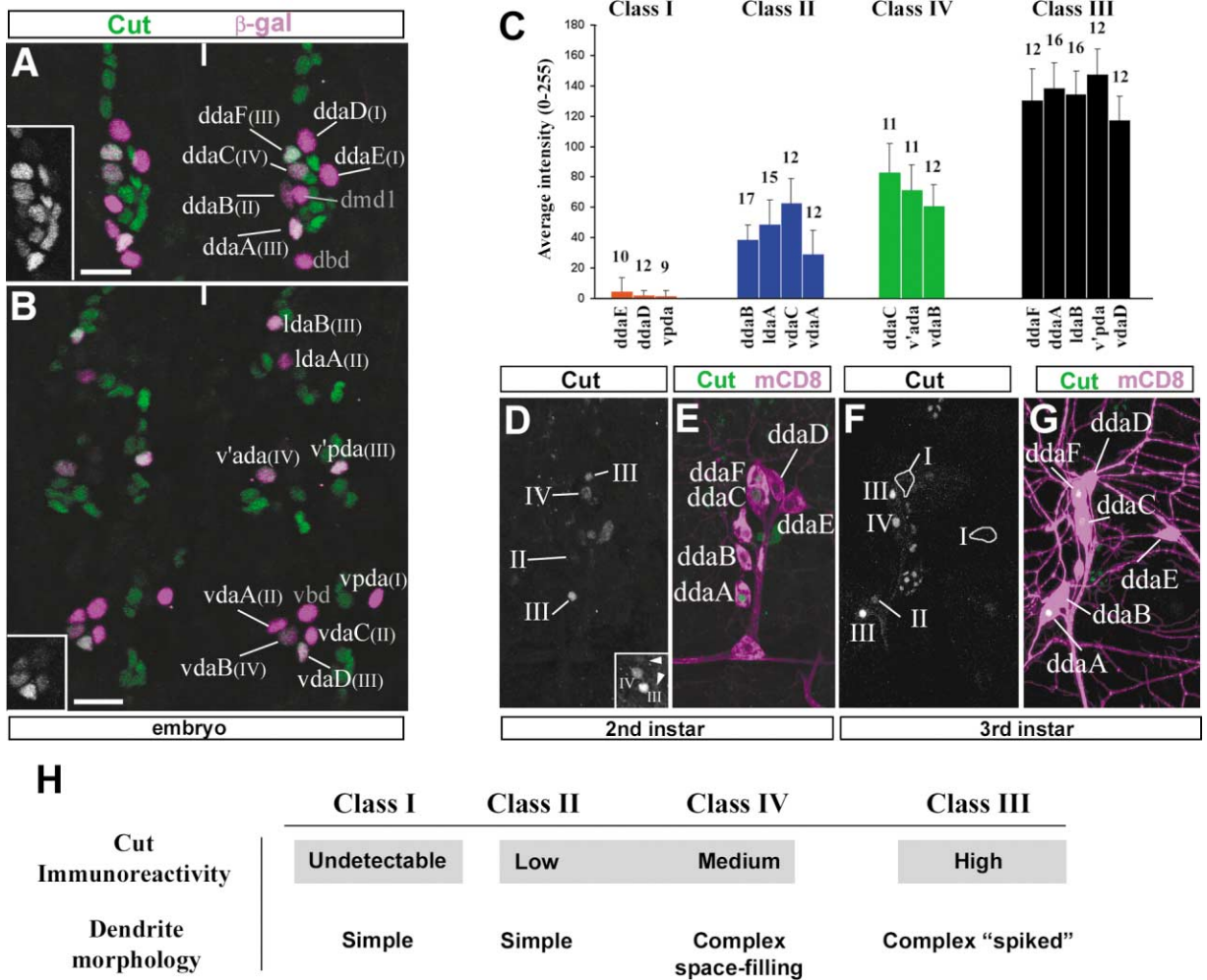
Figure 2. *cut* Expression in Embryonic and Larval da Neurons

(A) Anti-Cut (F2 antibody) staining (green) of embryonic dorsal cluster in two adjacent segments. Segments are separated by an upper tick mark. Multidendritic neurons labeled by the *E7-2-36* enhancer trap are magenta. Names of da neurons are white and provided with their designated class (I–IV). Names of non-da multidendritic neurons are shaded gray. es neurons and their support cells are labeled with Cut, but not β-gal, antibodies. Inset: single channel image of the Cut label of da neurons. Dorsal is up and anterior is to the left in this and all subsequent panels. Scale bar = 20 μm.

(B) Ventral and lateral clusters stained for Cut (green) and *E7-2-36* enhancer activity (magenta). Segments are separated by an upper tick mark. Inset: single channel image of ventral cluster Cut label. Scale bar = 20 μm.

(C) Quantification of Cut immunoreactivity (measured as mean pixel intensity) in stage 16 embryonic da neurons. Numbers are cells measured.

(D) Expression of Cut in the dorsal cluster of a second instar larva. Class II, III, and IV neurons are indicated. Inset: cut antibody labeling of ventral cluster class II (arrowheads), III, and IV neurons.

(E) *Gal4[109(2)80]*-driven *mCD8::GFP* (magenta) merged with Cut (green) with the identities of each neuron indicated. Anti-Cut was imaged in the red channel and anti-mCD8 in the green channel but switched during processing to maintain consistency with (A) and (B).

(F) Expression of Cut in the dorsal cluster of a third instar larva. Cut-positive da neurons are indicated according to their morphological class (II, III, or IV). Cell bodies of class I neurons are outlined.

(G) *Gal4[109(2)80]*-driven *mCD8::GFP* (magenta) merged with Cut (green). Anti-Cut was imaged in the red channel and anti-mCD8 in the green channel but switched during processing to maintain consistency with (A) and (B).

(H) Summary of Cut levels and dendrite morphologies of da neurons. Gray boxes indicate significantly different levels for all cells within the group in embryos.

"td" neuron of Gao et al., 1999). These results indicated that *ASC*-dependent da neurons are distributed in all four morphological classes.

cut Expression in the da Neurons

The selector gene *cut* acts in *ASC*-dependent lineages to specify cell identity (Blochlinger et al., 1991) and is expressed at different levels in various embryonic da neurons (Blochlinger et al., 1990). We examined *cut* expression in embryonic stages to determine the relationship, if any, between these levels and the morphological categories proposed for the da neurons (Grueber et al., 2002). We used Cut antibodies directed against a C-terminal protein (Blochlinger et al., 1988, 1990) to stain embryos of the enhancer line *E7-2-36* (which bestows all md neurons with *lacZ* expression). We found that
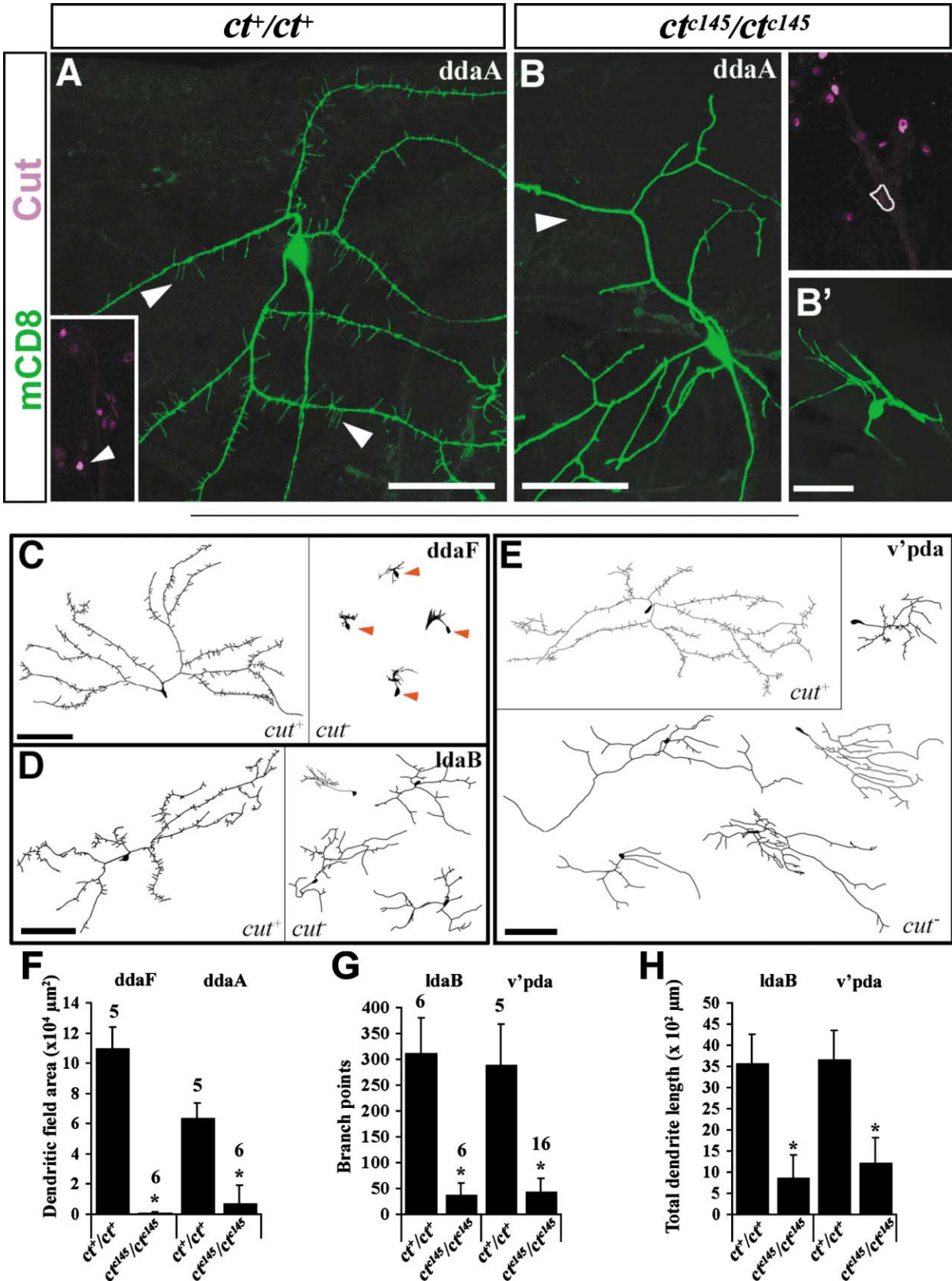
Figure 3. *cut* Mutant Phenotype of Class III Neurons

(A) Class III neurons (ddaA shown here) show extensive protrusions or dendritic spikes (arrowheads) extending from each major dendrite branch. Inset, high Cut expression in class III neurons (small arrowhead; the same neuron marked with GFP). Dorsal is up and anterior is to the left in this and all subsequent panels. Scale bar = 50 μm for (A)–(B′).

during embryonic stages, most da neurons express Cut but at different levels (Figures 2A and 2B). These levels were serially repeated in each abdominal segment (thoracic segments were not examined) and showed a close correlation with morphological class (Figure 2C). Cut immunoreactivity was high in class III neurons, which show many short dendritic spikes; medium in the class IV neurons, which have expansive and highly complex arbors, and in the sparsely branching class II neurons; and below detection in the simple class I neurons (Figure 2C).

Cut is expressed in sense organ precursors and their progeny, consistent with a role in identity specification (Blochlinger et al., 1990; Figures 2A and 2B). However, an intriguing aspect of *cut* expression is that it persists in postmitotic cells (Blochlinger et al., 1990, 1993). To examine Cut expression in da neurons at larval stages, we labeled both a wild-type strain and $Gal4^{109(2)80}$, UAS-*mCD8::GFP* heterozygotes with a Cut antibody directed against an N-terminal peptide (Blochlinger et al., 1988). We examined second and third instar larval stages and found that as in embryos, *cut* was expressed in class II, III, and IV neurons and was not detected in class I neurons (Figures 2D–2G). The relative levels seen in larval neurons were the same as in embryos (Figures 2A and 2B), although at these later stages, staining in class IV neurons appeared stronger than in the class II neurons (Figures 2D–2G). Thus, neurons showing the highest Cut levels throughout embryonic and larval development matched those that exhibit short dendritic spikes along their main trunks (Figure 2H), while relatively lower levels were associated with class IV and class II morphologies. These results suggested that Cut might be a good candidate for a regulator of class-specific properties of dendrites.

Single-Cell Analysis of *cut* Function in Class III Neurons

The *cut* locus is large, and mutations showing embryonic and adult phenotypes fall into five groups (Jack, 1985; Blochlinger et al., 1988; Liu et al., 1991). Mutations that disrupt the coding region (the lethal II group; Jack, 1985) affect cell fate decisions in external sensory organs of the PNS and are embryonic lethal (Bodmer et al., 1987; Blochlinger et al., 1988). For initial experiments to examine the role of Cut in dendrite morphogenesis, we examined embryonic phenotypes using pan-da markers, such as *elav-Gal4* and $Gal4^{109(2)80}$. These experiments suggested that arbors became simplified in *cut*⁻ embryos (data not shown); however, embryonic lethality and labeling of many neurons together limited our ability to

resolve the phenotype. We therefore explored the changes to dendrite morphology caused by loss of Cut at the level of single identifiable neurons. We used the MARCM system (Lee and Luo, 1999) to generate mCD8::GFP-labeled *cut* homozygous mutant neurons in an otherwise heterozygous *cut* background. We recombined two lethal II group *cut* alleles, ct^{c145} and ct^{db3}, into different MARCM configurations and used heterozygous $Gal4^{109(2)80}$, which labels da neurons, bipolar neurons, cells of the chordotonal organ, and oenocytes (Gao et al., 1999), to mark our mutant clones. ct^{c145} and ct^{db3} are considered null alleles (Jack, 1985; Blochlinger et al., 1988).

We focused our analysis first on neurons that consistently showed the highest levels of Cut immunoreactivity, the class III neurons, reasoning that these might show the most dramatic phenotypes. We obtained clones of each of the five class III neurons, and indeed all showed dendrite branching and elongation phenotypes (n = 49). The phenotypes were of two broad categories. Dendrites of both dorsal cluster neurons, ddaA and ddaF, showed a dramatic defect in higher-order branching and elongation, resulting in a highly reduced dendritic field (Figures 3A–3C and 3F). ddaA showed slightly less extreme phenotypes than ddaF, and examination of the dendritic trunks of ddaA revealed an absence of the "spikes" that distinguish the class III neurons (Figures 3B and 3B′). ldaB occasionally showed a severe growth phenotype similar to ddaF and ddaA (4 of 15 clones examined) but more often fell into the second category of phenotypes, which was an absence or severe reduction of dendritic spikes with only partially reduced primary dendritic trunks (Figure 3D). A lack of spikes was also the dominant phenotype of v'pda (Figure 3E) and vdaD (data not shown). These phenotypes resulted in a significant reduction in total dendritic length and number of branch points (Figures 3G and 3H). When standardized to total dendrite length, the decrease in branching remained significant (p < 0.05; Wilcoxon two-sample test), indicating that the effect on branching is not a secondary consequence of decreased dendrite elongation. These data supported a crucial role for Cut in the acquisition of the class-specific spiked morphology of the class III neurons.

cut Regulation of Morphogenesis in Dorsal Class IV, II, and I Neurons

Other da neurons that do not have the spiked dendrite morphology of the class III neurons showed relatively weaker labeling with Cut antibodies (Figure 2). Focusing primarily on the dorsal cluster because of the larger

(B and B′) Lacking Cut, the class III neuron ddaA shows few of its characteristic protrusions (arrowhead) and a reduced dendrite elongation (B′). Inset, Cut label of the dorsal cluster with the ddaA clone outlined. Clone genotype: $w\ ct^{c145}\ FRT^{19A}/w\ ct^{c145}\ FRT^{19A}$; $Gal4^{109(2)80}$, UAS-*mCD8::GFP/+*.

(C) *cut*⁺ clone of ddaF (left) and phenotypes of several *cut*⁻ ddaF clones (right). *cut*⁻ clones shown in (C)–(E) were made using the ct^{c145} allele. Scale bar = 100 μm.

(D) *cut*⁺ clone of ldaB (left) and the phenotypes of several *cut*⁻ ldaB clones (right). Scale bar = 100 μm.

(E) *cut*⁺ clone of v'pda (left) and the phenotypes of several *cut*⁻ v'pda clones (right). Scale bar = 100 μm.

(F) Quantification of dendritic field area for ddaA and ddaF in *cut*⁺ and *cut*⁻ clones.

(G) Quantification of number of branch points for ldaB and v'pda in *cut*⁺ and *cut*⁻ clones.

(H) Quantification of total dendrite length for ldaB and v'pda in *cut*⁺ and *cut*⁻ clones. Asterisks in (F)–(H), p < 0.05 (Wilcoxon two-sample test).
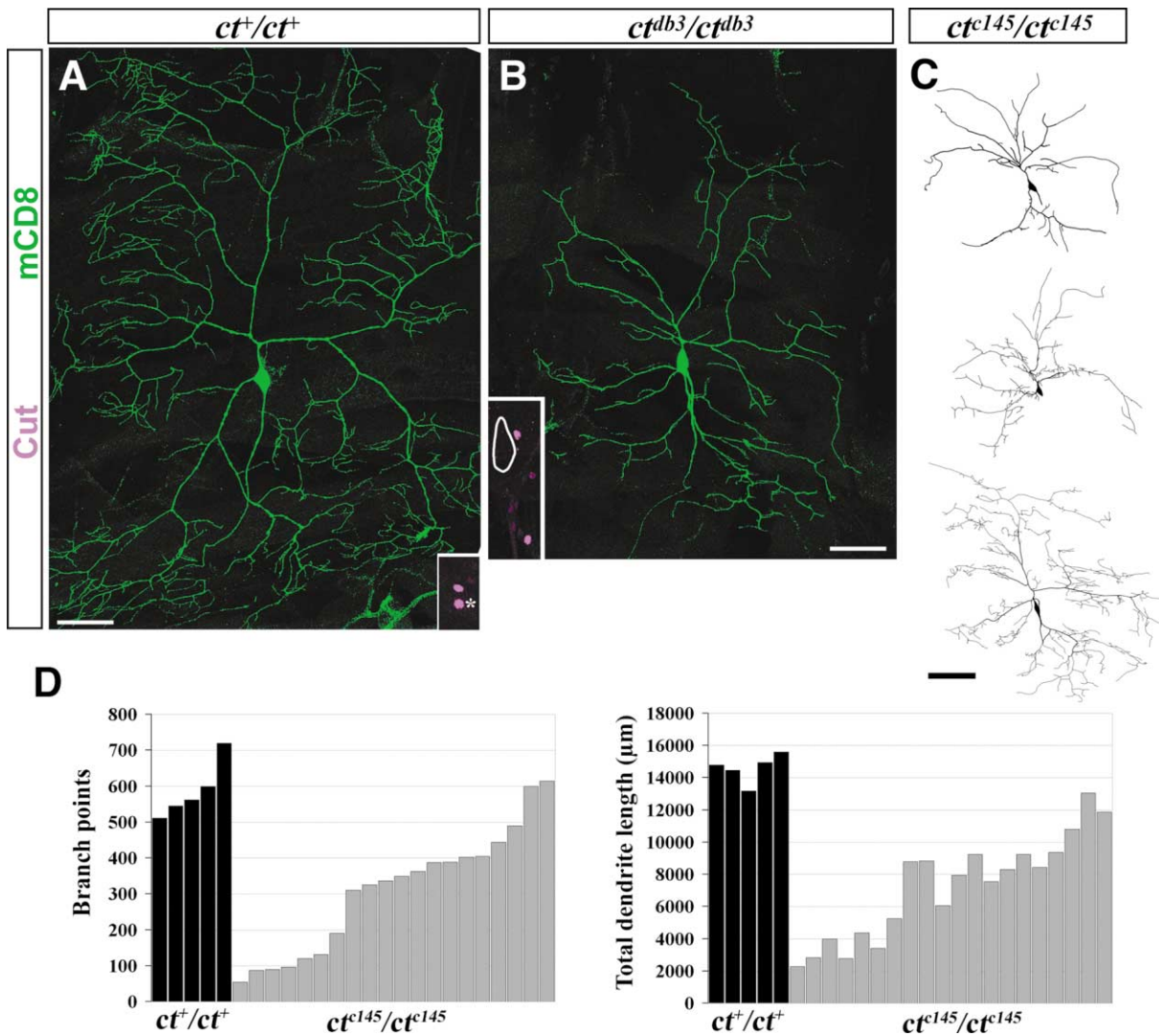
Figure 4. *cut* Mutant Phenotype of the Class IV Neuron ddaC

(A) MARCM clone of the class IV neuron ddaC. Inset shows Cut antibody labeling with the Cut-positive nucleus of ddaC indicated with an asterisk. Clone genotype: *y w FRT[19A]/y w FRT[19A]*; *Gal4[109(2)80]*, UAS-*mCD8::GFP/+*. Dorsal is up and anterior is to the left in this and all subsequent panels. Scale bar = 50 μm.

(B) *cut[−]* class IV neuron, ddaC, does not extend dense branches to cover the epidermis. Inset shows lack of Cut antibody staining in the mutant ddaC neuron (oval). Two adjacent class III neurons express high levels of Cut. Clone genotype: *y w ct[db3] FRT[9−2]/y w ct[db3] FRT[9−2]*; *Gal4[109(2)80]*, UAS-*mCD8::GFP/hsFLP*. Scale bar = 50 μm.

(C) Range of ddaC branching phenotypes using the *ct[c145]* allele (*ct[db3]* gave a similar range). For reference, a *cut[+]* clone is traced in Figure 1F. Scale bar = 100 μm.

(D) Distribution of number of branch points (left) and total dendritic length (right) for control clones (black bars) and mutant clones made with the *ct[c145]* allele (gray bars), showing the variability of ddaC phenotypes. Each bar represents data from a single individual neuron. The order of the neuron from left to right is maintained in both graphs.

number of clones obtained from this region, we examined whether Cut might regulate morphogenesis also in these low-level neurons. The class IV neuron ddaC normally innervates a large region of the body wall with a highly branched arbor (Figure 4A). We found that in *cut[−]* clones, ddaC showed decreased dendrite branching and elongation (Figure 4B) and that the severity of these defects was highly variable from cell to cell. The most severely affected neurons extended a "skeleton" of the normal class IV arbor with a complete loss of higher-order branches and a reduced overall dendrite length

(Figures 4C and 4D), suggesting that Cut regulates the terminal branching pattern of these cells. The least affected neurons showed a degree of branching comparable to control neurons (Figures 4C and 4D). A similar range of phenotypes was observed in the two ventral class IV neurons (data not shown). Given the frequent strong branching and elongation defects (Figures 4C and 4D) and the expression of Cut in sensory precursor cells (Blochlinger et al., 1988, 1990), the variation in clone phenotype might be due to perdurance of wild-type protein (see Lee and Luo, 1999; Lee et al., 2000).
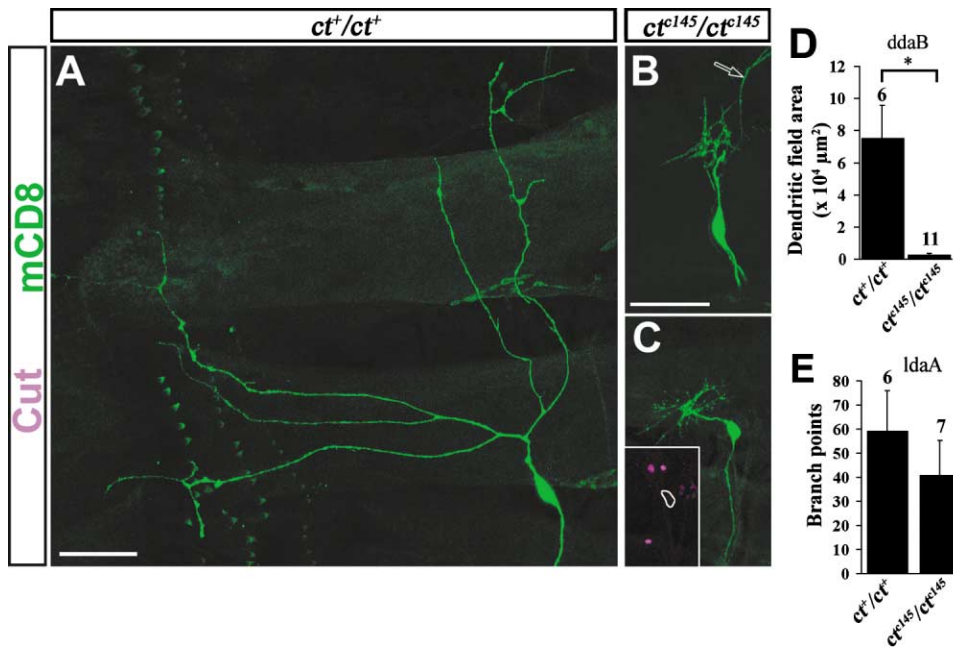
Figure 5. *cut* Mutant Phenotype of Class II Neurons

(A) A representative *cut*[+] class II neuron, ddaB. Clone genotype: *y w FRT[19A]/y w FRT[19A]; Gal4[109(2)80]*, UAS-*mCD8::GFP/*+. Dorsal is up and anterior is to the left in this and all subsequent panels. Scale bar = 50 μm.

(B) In *ct[c145]* clones, ddaB shows severely decreased dendrite elongation. The axon of a nearby neuron is indicated by a white arrow. Clone genotype: *w ct[c145] FRT[19A]/w ct[c145] FRT[19A]; Gal4[109(2)80]*, UAS-*mCD8::GFP/*+. Scale bar = 50 μm.

(C) A ddaB *cut* mutant clone (green) costained with Cut (inset) to identify the neuron based on its position relative to other dorsal neurons. ddaB is flanked by strongly labeled class III and class IV neurons. Same genotype and same scale as in (B).

(D) Quantification of dendritic field area in *cut*[+] and *cut*[−] clones. Asterisk, $p < 0.05$ (Wilcoxon two-sample test).

(E) Quantification of number of branch points for ldaA in *cut*[+] and *cut*[−] clones.

The class II neurons normally label weakly with Cut antibodies (Figure 2) and extend expansive, yet sparsely branched arbors (Figure 5A). The dorsal cluster class II neuron ddaB showed a severe and completely penetrant decrease in dendrite growth in *cut*[−] clones (n > 15; Figures 5B–5D). The final form of mutant clones resembled the typical mutant phenotype of the dorsal cluster class III neurons, ddaA and ddaF, with a single dorsal branch that ended as a tuft of dendrites immediately anterior to the dorsal cluster. Among the class II neurons, this severe growth phenotype was specific to ddaB (n = 14). ldaA and the ventral neurons showed variable reductions in branching in *cut*[−] clones compared to controls (Figure 5E; $p < 0.1$ for ldaA, $p < 0.05$ for ldaA, vdaC, and vdaA pooled; Wilcoxon two-sample test). Considering the already sparse dendrites extended by these neurons and the possibility of Cut perdurance in mutant clones, these results together suggest that Cut expressed in ddaB and also in other class II neurons is important for proper dendrite branching.

The two dorsal class I neurons, ddaD and ddaE, showed normal dendrite morphologies in mutant clones (n > 20; Figures 6A and 6B), and quantification of the average number of branch points and total dendritic length of the two dorsal neurons revealed no significant differences from control clones (Figures 6C and 6D). These results are consistent with the lack of detectable Cut immunoreactivity in both cells.

In summary, our clonal analysis indicated that Cut is required for a terminal branching morphology specific to the class III sensory neurons and for the normal morphology of neurons that show lower levels of Cut immunoreactivity. Neurons that show no detectable Cut expression showed no such requirement.

Effect of *cut* Ectopic Expression in Neurons that Normally Lack Cut

Based on the patterns of *cut* expression in the da neurons (Figure 2) and the loss of function phenotypes, class-specific dendrite branching could be regulated by different levels of Cut activity. More specifically, high levels of Cut might lead to dendrites with numerous short terminal branches (i.e., spikes), while maintaining low levels in neurons may lead to simpler arbors. We tested this hypothesis first by expressing *cut* ectopically in neurons with simpler branch morphologies that normally lack detectable Cut protein. The class I neurons typically extend few fine dendritic branches, and in later larval instars these were often stable over the course of 1–2 days (n = 17; Figures 7A and 7A′). We found that Gal4-induced ectopic expression of *cut* in these neurons, beginning late in embryogenesis, caused a completely penetrant acquisition of exuberant short dendritic branches (n > 300 cells examined; Figure 7B). Ectopic branching was apparent by the first instar stage (data not shown) and persisted throughout larval development. Monitoring of cells over time revealed that these terminal branches were highly dynamic (n = 25;
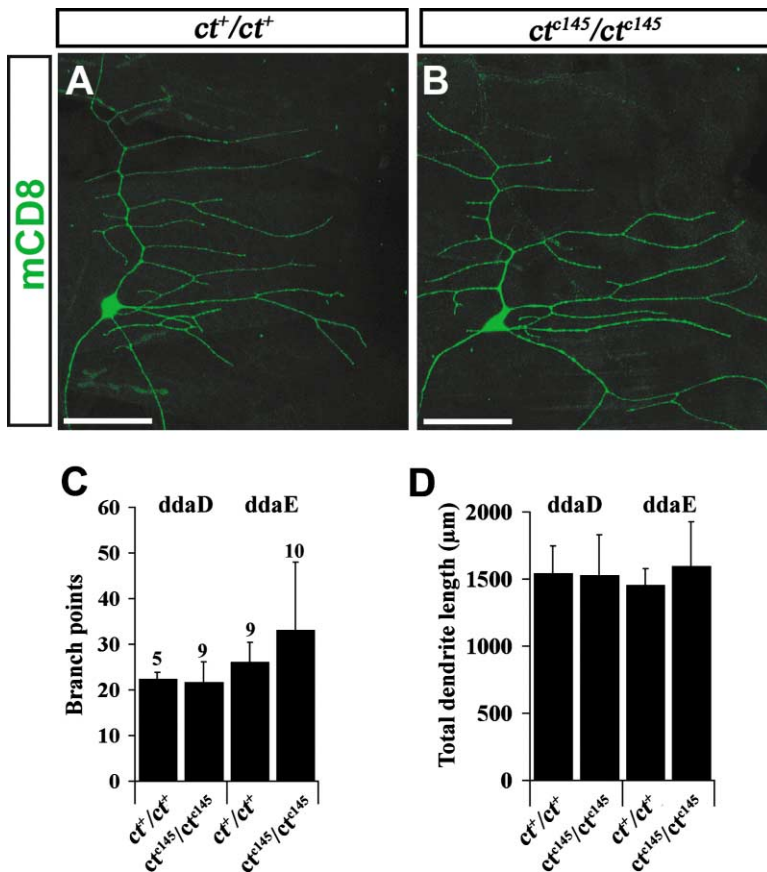
Figure 6. Lack of Detectable Phenotype in *cut* Mutant Dorsal Class I da Neurons

(A) A *cut*⁺ clone of the class I neuron, ddaE. Clone genotype: *y w FRT¹⁹ᴬ/y w FRT¹⁹ᴬ; Gal4¹⁰⁹⁽²⁾⁸⁰, UAS-mCD8::GFP/+*. Dorsal is up and anterior is to the left in this and all subsequent panels. Scale bar = 50 μm.

(B) ddaE shows a normal dendrite morphology in *cut⁻* clones. Clone genotype: *w ct^c145 FRT¹⁹ᴬ/w ct^c145 FRT¹⁹ᴬ; Gal4¹⁰⁹⁽²⁾⁸⁰, UAS-mCD8::GFP/+*. Scale bar = 50 μm.

(C) Quantification of number of branch points for ddaD and ddaE.

(D) Quantification of total dendrite length for ddaD and ddaE.

Figure 7B′). At successive time periods spaced over 2 days, we identified apparently stable branches of various lengths, branches that had shortened, and branches that had grown or appeared de novo. As was observed in neurons not expressing Cut ectopically (Figure 7A′), the pattern of major trunks was stable (Figure 7B′). A significant but less extreme overbranching was induced by forced expression of CCAAT-displacement protein (CDP), a human homolog of *Drosophila cut* (n > 40 cells examined; Figures 7C and 7D; Neufeld et al., 1992).

Loss-of-function studies provided evidence that Cut controls dendritic elongation (Figures 3 and 4) and gain-of-function phenotypes provided further support for such a role. Class I neurons ectopically expressing Cut or CDP showed a larger dendritic field and greater total dendrite length than control neurons (Figure 7D). Furthermore, each class I neuron extended dendrites beyond the segment borders when forced to express Cut. In this respect, these arbors were distinct from the dendrites typical of class I neurons, which terminate within segments (Figure 7A; Grueber et al., 2002), and more like the highly branched dendrites of class III and class IV neurons, which can cross segment boundaries.

Effect of *cut* Overexpression in Low-Level and Medium-Level Neurons

Because Cut is normally not detected in the class I neurons, the above results do not address whether Cut acts as a binary on-off switch to induce dendrite branching and elongation or in a level-dependent fashion. To examine this issue, we tested the effect of boosting Cut levels in dorsal cluster class II and class IV neurons. These neurons normally showed low and medium levels of Cut, respectively, and required Cut for proper dendrite morphogenesis (Figures 4 and 5). If different Cut levels contribute to class-specific morphogenesis, then the sparse branching of class II neurons and the long terminal branches of class IV neurons might be augmented or replaced by the type of short spikes that characterize high-expressing neurons. Lacking a class-II-specific driver, we used *Gal4¹⁰⁹⁽²⁾⁸⁰* to drive *mCD8::GFP* and uniformly high levels of Cut in all dorsal da neurons and then selectively visualized the class II neuron ddaB by ablating all other neurons except for this one and the dmd1 neuron (which lies immediately dorsal to ddaB and aided in its identification). Following the cell ablations, larvae were recovered and left to develop for 1–2 days before immunolabeling to examine dendrite morphology and Cut expression. Laser ablation was specific to those cells targeted and in control animals revealed the full normal morphology of ddaB (n = 9 cells; Figure 8A). When Cut was driven to high levels, dendrites were transformed to a highly branched morphology with more numerous and dense short terminal spikes extending from main branches (Figures 8B–8D, n = 12). To examine whether class IV neurons also acquire an alternate morphology in response to Cut overexpression we used a class IV-specific *Gal4* line, *Gal4⁴⁷⁷*
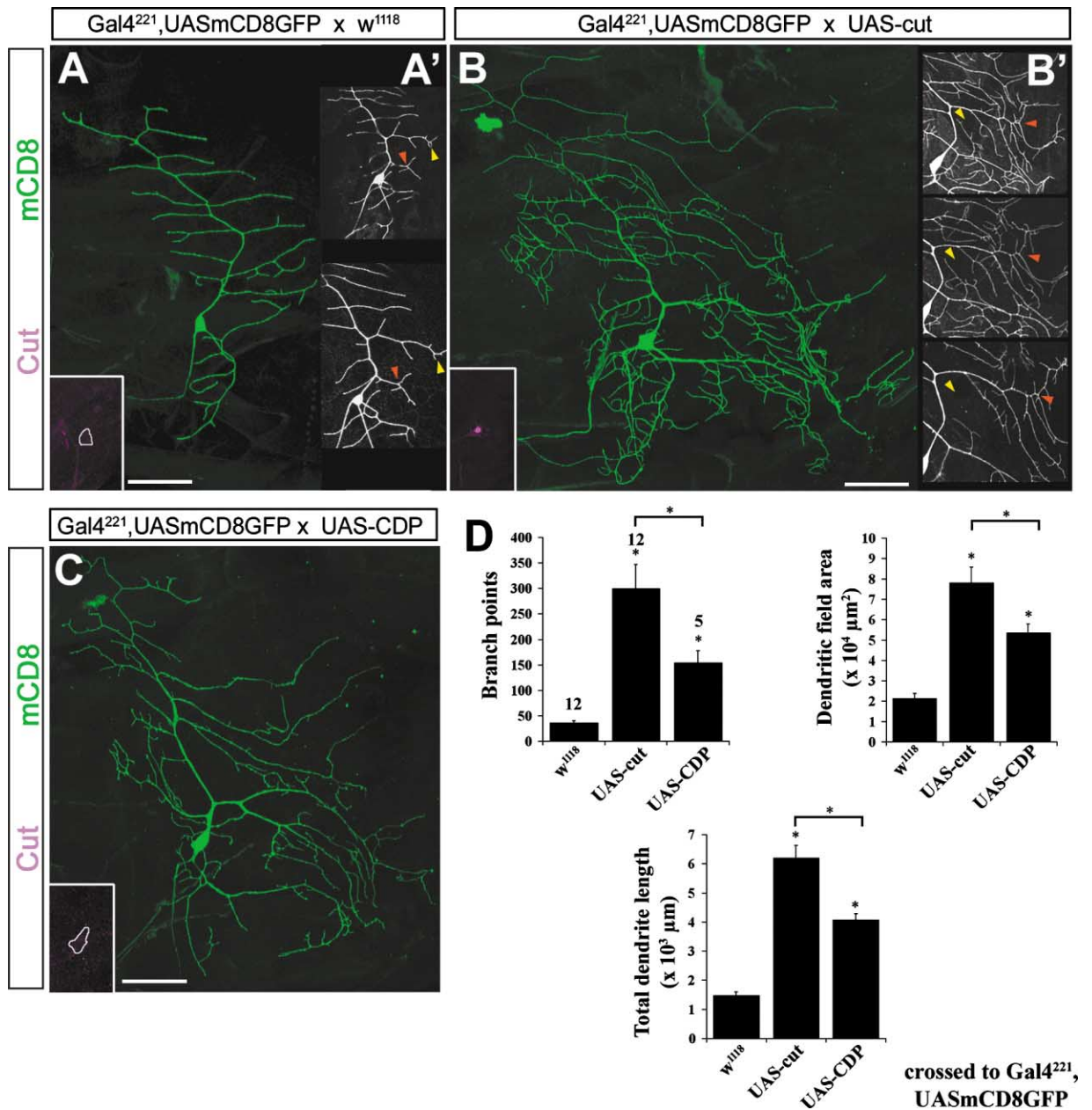
Figure 7. Effect of *cut* Ectopic Expression on Class I Neuron Dendrite Morphology

(A and A′) *Gal4²²¹*-driven *mCD8::GFP* in the ventral class I neuron, vpda. (A′) 24 hr time lapse of vpda dendrites beginning in second instar larva reveals little remodeling of fine dendrites. Yellow arrowhead indicates an example of a remodeling terminal, and a red arrowhead indicates apparently stable branches. Images in (A) and (A′) are not of the same neuron. Dorsal is up and anterior is to the left in this and all subsequent panels. Scale bar = 50 μm in (A).

(B and B′) Outgrowth and branching phenotype induced by *Gal4²²¹*-driven *cut* expression. Note the the extensive branching from the lateral dendritic trunks. (B′) Time lapse of arbors starting in mid-second instar stage (top) and imaged 15 (middle) and 40 (bottom) hr later reveals dynamic growth and branching of some arbors (yellow arrowheads) and relative stability of others (red arrowheads). Images in B and B′ are not of the same neuron. Scale bar = 50 μm in (B).

(C) Outgrowth and branching phenotype induced by *Gal4²²¹*-driven CDP expression.

(D) Quantification of the number of branch points, total dendritic length, and dendritic field area for control, Cut-expressing, and CDP-expressing class I neurons. Asterisks, $p < 0.05$ (Wilcoxon two-sample test).

to drive high levels of Cut beginning late in embryogenesis. In contrast to the normal long and sinuous terminal dendrites shown by class IV neurons (Figure 8E), overexpression of Cut induced significantly shorter terminals with both spiked and curved morphologies (n = 1796 terminals; Figures 8F and 8G). Cut overexpression in class III neurons produced no obvious defects in terminal branching (data not shown).
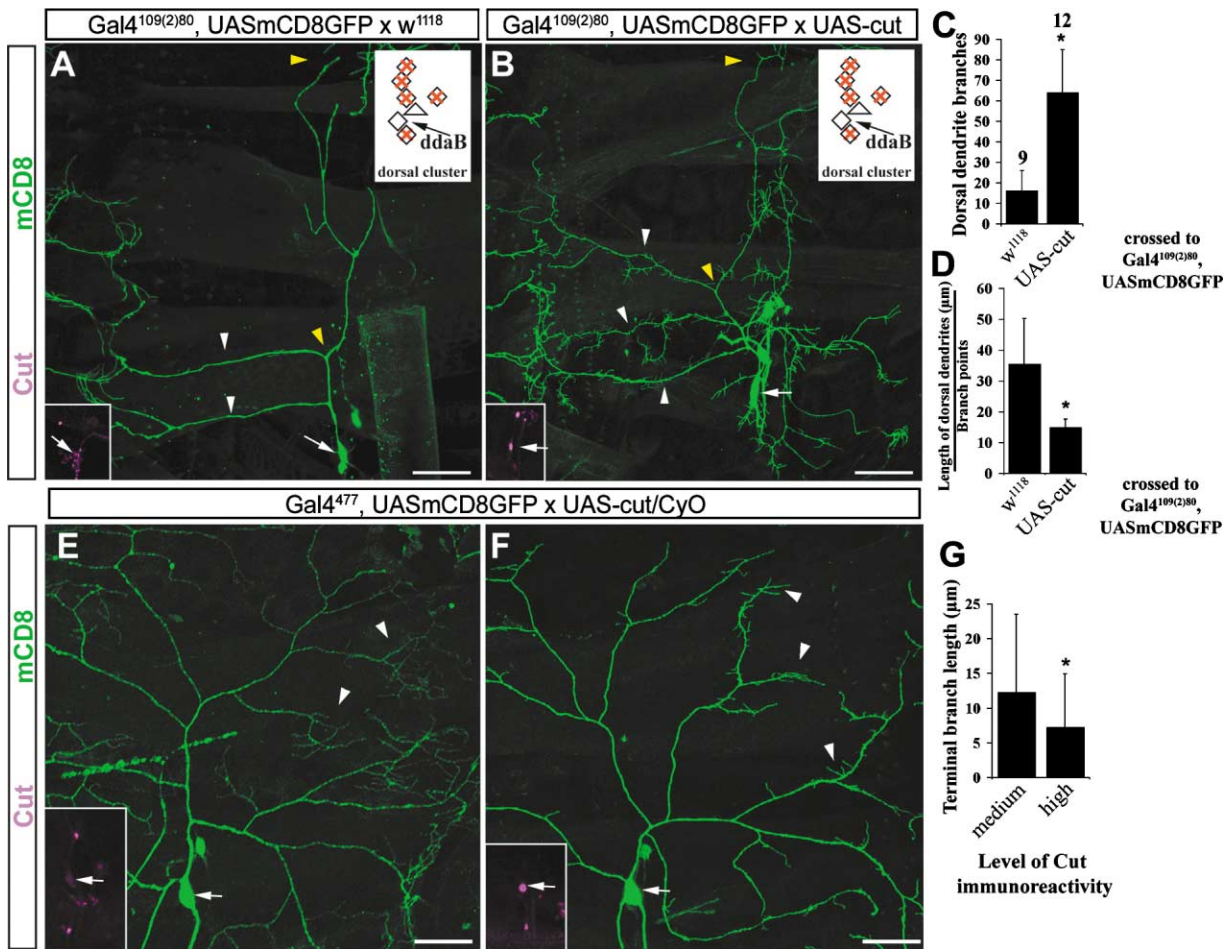
Figure 8. Effect of *cut* Overexpression on Class II and Class IV Neuron Morphologies

(A) Normal morphology of the class II neuron, ddaB after ablation of surrounding dorsal cluster da neurons (see upper inset). The cell body is indicated by an arrow and major anterior dendritic arbors by white arrowheads. Yellow arrowheads bracket the dorsal directed branch from which quantitative data were collected. Lower inset: Cut immunolabel showing low levels of fluorescence in ddaB (arrow). Dorsal is up and anterior is to the left in this and all subsequent panels. Scale bar = 50 μm.

(B) Morphology of ddaB expressing Cut under the control of the *Gal4^109(2)80*. Other dorsal da neurons were ablated as in (A), upper inset. A white arrow indicates the cell body of ddaB, white arrowheads point to ectopic branching of anterior arbors, and yellow arrowheads bracket the dorsal arbor from which quantitative data were collected. Inset: Cut immunolabel showing high level of staining in ddaB (arrow). Scale bar = 50 μm.

(C) Quantification of the number of branches on the dorsal dendrite. Asterisks, $p < 0.05$ (Wilcoxon two-sample test).

(D) Dorsal dendrite length divided by number of branch points. Asterisks, $p < 0.05$ (Wilcoxon two-sample test).

(E) ddaC neuron expressing *mCD8::GFP* under the control of one copy of *Gal4^477* showing the normal branching pattern. An arrow points to the cell body that labels moderately for Cut protein (inset) and arrowheads indicate fine branches.

(F) ddaC expressing high levels of Cut arising from *Gal4^477*,UAS-*mCD8::GFP* -driven UAS-*cut*. An arrow points to the Cut-positive nucleus (see inset) and arrowheads point to some of the many short branches that extend from the main dendritic trunks.

(G) Quantification of change in terminal branch length upon ectopic expression of Cut. Asterisks, $p < 0.05$ (Wilcoxon two-sample test).

Because Cut is observed at low to moderate levels in the dorsal class II and IV neurons and also required in these cells for proper dendritogenesis (Figures 4 and 5), these overexpression studies argue against binary regulation by Cut. Instead, it appears that the particular levels of Cut expressed by different da neurons are essential for their class-specific morphology.

Discussion

We have addressed how different classes of neurons can acquire stereotyped dendrite branching patterns during development by focusing on the regulation of da sensory neuron morphogenesis by the Cut homeoprotein. Previous reports suggested that different da neurons express different levels of Cut (Blochlinger et al., 1990). The distribution of neurons showing these different levels appeared to correlate with distinct morphological properties of dendrites (Grueber et al., 2002), which we explicitly examined by immunolabeling of embryonic and larval stages. We found that the highest levels of immunoreactivity were consistently shown by neurons sharing a common morphological property, namely short spikes extending from main dendritic trunks. Other

classes of neurons showed either medium to low levels of Cut (class IV and class II, respectively) or levels that were below the limit of detection (class I). Our conclusions regarding Cut levels are based on multiple criteria, including matching results with antibodies directed against either N-terminal or C-terminal regions of Cut, a reproducible staining pattern in multiple body segments (Figures 2A and 2B), and consistent levels of intensity within independently-derived morphological classes of neurons. Thus, although levels of immunoreactivity might not provide a linear readout of protein levels and do not necessarily reflect differences in activity, these considerations supported the notion that different levels of Cut might be important for establishing morphological distinctions between da neurons.

Given the expression patterns of Cut described above, we hypothesized that high Cut directs the production of more complex arbors, perhaps specifically the dendritic spikes shown by the class III neurons, and that low levels lead to simpler dendrites. Results from loss-of-function and gain-of-function manipulations provided strong support for this scenario and suggest that different levels of Cut direct different patterns of dendrite morphogenesis. First, in cut^- clones, class III neurons showed severe reductions in their class-specific spikes and resembled simpler skeletons of their normal arbor (Figure 3). Conversely, ectopic expression of Cut in nonexpressing neurons and in lower-level neurons initiated the branching of numerous spiked structures from their main dendritic trunks, causing these dendrites to take the appearance of class III arbors (Figures 7 and 8). Thus, these classes of neurons are capable of extending class III-like spiked dendrites, but for the class II and class IV neurons, the levels of Cut that direct their proper morphogenesis apparently fall below a required threshold. Considering that Cut is also required for proper dendritogenesis in class IV and class II neurons (Figures 4 and 5), it might regulate class-specific traits not only in class III neurons, but also in other neurons when expressed at lower levels.

Our results raise potential parallels for Cut action in es organs and da neurons. Merritt (1997) suggested that several distinctions between es and ch sensory organs could result from changes to the program specifying dendritic growth, in particular an enhanced growth of the outer dendritic segment of Cut-positive es neurons relative to Cut-negative ch neurons. Differential growth of these dendrites would likely, in turn, influence the shape and position of support cells and cuticular structures (Merritt, 1997). In the da neurons, several of the morphological differences between neurons likely entail changes in the relative extent of dendrite elongation and branching and/or branch stabilization–programs that, according to gain-of-function and loss-of-function results, appear to be regulated by Cut. Thus, *cut* may provide a promising nodal point for examining how diverse dendrite morphologies are established among different groups of *Drosophila* sensory neurons.

Does Cut specify cell identity among the da neurons or, rather, selectively control dendrite morphogenesis? Homeodomain transcription factors, including Cut, have well-established roles in cell fate specification (Blochlinger et al., 1988; Briscoe et al., 2000; Jessell, 2000).

However, transcription factors expressed at later stages of differentiation can selectively control fine aspects of morphogenesis (Arber et al., 2000; Mollereau et al., 2001; Livet et al., 2002). For example, in *Drosophila* photoreceptor formation, the *spalt* gene complex controls rhabdomere morphology and *opsin* gene expression, but not axon projection pattern (Mollereau et al., 2001). Conversely, the *runt* transcription factor controls a subset of axon projection patterns without altering the expression of numerous markers of cell identity (Kaminker et al., 2002). The expression of Cut in both sensory precursors and differentiated neurons, together with studies of *cut* function in the PNS, suggest that it might control both the identity and later development of da neurons (Blochlinger et al., 1990; Brewster and Bodmer, 1995; Brewster et al., 2001; this study). If Cut does generally specify da neuron fate, then our ability to transform dendrite morphology by postmitotic expression of Cut argues that this aspect of identity is not established in an all-or-nothing fashion at the time of neuronal birth.

Because the Cut protein contains several DNA binding motifs (including a homeodomain and three Cut repeats; Blochlinger et al., 1988) and is localized to the nucleus, it likely controls dendrite morphology through transcriptional regulation. Such a mechanism of action is supported by the ability of mammalian *cut* homolog with conserved DNA binding domains (Neufeld et al. 1992; Andres et al., 1994; Nepveu, 2001) to partially rescue Cut loss-of-function (Ludlow et al., 1996) and induce growth of da neuron dendritic arbors (Figure 7). Although level-dependent regulation of dendrite morphology by homeoproteins has, to our knowledge, not previously been demonstrated, level-dependent control of cell identity by homeoproteins has been shown in both nonneuronal and neuronal systems (Driever and Nüsslein-Volhard, 1988b; Struhl et al., 1989; Vallstedt et al., 2001). Bicoid, for example, is distributed in a morphogen gradient along the anterior-posterior axis of the syncytial *Drosophila* embryo (Driever and Nüsslein-Volhard, 1988a) and can exert threshold-dependent effects on gene expression by cooperative DNA binding (Burz et al., 1998), which may be an important mechanism of target gene activation as the embryonic body pattern is organized. The identities of transcriptional targets of Cut in the embryonic and larval PNS are not yet known. Based on the present results, Cut could control the expression of key regulators of dendrite branching.

cut homologs have been identified in several vertebrates, including human, dog, chick, and mouse (Neufeld et al., 1992; Andres et al., 1992; Valarché et al., 1993; Yoon and Chikaraishi, 1994; Quaggin et al., 1996). The ability of a mammalian *cut* homolog to regulate dendrite development in *Drosophila* raises the possibility of conserved roles in regulating neuronal morphogenesis. Indeed, of the two murine *cut* homologs, *Cux-1* is expressed in many adult tissues including the nervous system, while *Cux-2* is expressed solely in the developing and adult nervous system (Valarché et al., 1993; Quaggin et al., 1996). In embryonic stages, *Cux-2* is expressed in the telencephalon, trigeminal ganglion, and spinal cord (Quaggin et al., 1996). In the adult, strong expression is observed in the thalamus, pyramidal neurons of the hippocampus, the granule cell layer of the

dentate gyrus, and amygdala, while lower levels are seen in the cerebral cortex (Quaggin et al., 1996). Based on such widespread distribution in the mammalian central and peripheral nervous system, it will be interesting to examine potential roles for *Cux* genes in cell identity specification and neuronal morphogenesis in vertebrates. Perhaps further studies of how Cut acts to regulate dendrite morphology in *Drosophila* will prove useful for dissecting this potentially important mechanism by which homeoproteins contribute to cellular diversity.

Experimental Procedures

Fly Stocks
We identified *ASC*-independent neurons using the stock *Df*(1)*sc*[B57] *w sn/FM6 y w B*; *Gal4*[109(2)80], UAS-*GFP*. We generated by standard genetic techniques and mated the following pairs of lines for MARCM analysis: (1) *tub-Gal80, hsFLP, FRT*[19A]; *Gal4*[109(2)80], UAS-*mCD8::GFP*/CyO to (2) *w ct*[c145] *FRT*[19A]/*y*[+]*ct*[+]*Y*, and (3) *y w ct*[db3] *FRT*[9-2]/*FM6*; *hsFLP*/+ to (4) *tub-Gal80, FRT*[9-2]/*Y*; *Gal4*[109(2)80], UAS-*mCD8::GFP* (kindly provided by Y. Hong, UCSF). Males of the genotype *y w FRT*[19A] were crossed to stock (1) above to provide *cut*[+] clones. Lines expressing *Gal4* in subsets of da neurons were identified from an enhancer trap screen (original stocks kindly provided by Dr. Ulrike Heberlein, UCSF), and UAS-*mCD8::GFP* was recombined onto the same chromosome as the insertion. For ectopic *cut* expression experiments, homozygous *Gal4*, UAS-*mCD8::GFP* flies were crossed to either *w*;UAS-*cut*[EHK2]/CyO, *w*;UAS-*cut*[EHK2]/CyO- *act-lacZ*, *w*;UAS-*cut* (remobilized by C. Micchelli; courtesy of R. Bodmer), or *w*;UAS-CDP (stocks kindly provided by R. Bodmer, K. Blochlinger, and S. Jackson). *w*[1118] flies crossed to the above *Gal4* lines produced control larvae.

MARCM Analysis and Immunocytochemistry
To generate MARCM clones, embryos were collected for 2 hr and allowed to develop for 3–5 hr at 25°C before providing a heat shock. The heat shock paradigm was 38°C for 45 min, followed by a room temperature recovery for 30 min, and 38°C for an additional 30 min. Late third instar larvae were examined for clones and then dissected, fixed, and processed according to the methods of Grueber et al. (2002). Because of the morphological changes caused by *cut* mutations, we verified neuronal identity by costaining all clones with rat anti-mCD8 (Caltag, Burlingame, CA) and either anti-Cut to identify according to position relative to Cut-positive neurons (Blochlinger et al., 1988; Blochlinger et al., 1990) or mAb 22C10 (Zipursky et al., 1984). For Cut immunolabeling, we used rabbit anti-Cut (clp2 antibody raised against an amino-terminal peptide), rat anti-Cut (F2 antibody raised against a carboxy-terminal protein), or mouse anti-Cut (F2) (Developmental Studies Hybridoma Bank) antibodies at 1:1000, 1:5000, and 1:20 dilutions, respectively, and 1:200 dilutions of the appropriate Cy2 or Rhodamine Red X-conjugated secondary antibody (Jackson Laboratories). Prior to staining, Cut antibodies were typically preabsorbed overnight against embryos. For double-labeling *E7-2-36* embryos, we used 1:5000 rabbit anti-β-gal, and 1:5000 rat anti-Cut F2 antibodies.

Quantitative Analysis
A total of 194 clones of *ct*[c145], *ct*[db3], and *ct*^{+} neurons, most collected at 40× magnification, were acquired on a Leica TCS SP2 confocal microscope and reconstructed as montages following the methods of Beck et al., (2000). These neurons were representative of all clones examined and were selected for reconstruction and quantification based on the quality of staining, lack of extensive folding of the underlying cuticle, and absence of damaged or broken branches. Dendrites were quantified as collapsed Z sections (these arbors approximate a 2D plane on the epidermis) using NIH Image 1.63 with scaling factors obtained from Leica confocal software. Representative neuronal tracings for figures were made using Adobe Photoshop 7.0 (Adobe Systems, San Jose) by adding a transparent layer to confocal images and tracing the arbors using a mouse. Data in graphs are presented as means ± SD. Statistical analysis was performed in S-Plus (Insightful Corporation, Seattle WA). Statistical

analyses were performed on individual neurons only when at least five MARCM clones (range 5–20) each were reconstructed for mutant and control. Quantification of class II arbors in ectopic expression experiments was performed on the dorsal-directed branch due to the extensive overlap of anterior-directed arbors with arbors from neurons in adjacent segments. Sampling of these anterior dendrites revealed no major differences from dorsal dendrites.

Cut immunofluorescence was quantified in *E7-2-36* embryos (to allow unambiguous identification of each neuron) double-labeled with rabbit anti-Cut (F2) and rat anti-β-galactosidase antibodies. All embryos were processed in a single batch. Images were collected on a Leica TCS SP2 confocal microscope in one sitting using a 40× objective as 1024 × 1024 0.5 μm Z sections at 500–535 Hz emission, minimum laser power, 500 gain, airy 1 pinhole (81.42 μ), and 3.5× zoom. Each neuron was identified in three adjacent sections of the Z series, and manually outlined in eight-bit mode in ImageJ (NIH) to obtain the average pixel intensity. The highest of these three values was taken as the intensity value for each cell. Because background levels might vary for different animals, we outlined random Cut-negative epidermal cells and subtracted these values from the raw intensity measurements. Cut staining was also examined qualitatively in Canton-S and *w*[1118] strains.

Cell Ablations
Second instar larvae were placed singly on a glass slide and covered with a small amount of Halocarbon oil (Series 27, Halocarbon Products Corp., Rivers Edge, NJ) and a 22 × 22 mm glass coverslip. Cells were ablated using a Micropoint Laser System (Photonic Instruments Inc., Arlington Heights, IL) with a 337 nm pulsed nitrogen laser. After the ablation, the slide was submerged in a dish of halocarbon oil so that the coverslip floated away or could be lifted with forceps without harm to the larva. Individual larvae were recovered, gently cleaned of oil, and allowed to develop 1–2 days to late third instar on a yeasted grape agar plate kept at 25°C at which time they were dissected and immunolabeled as described above.

Time Lapse Imaging
Second instar larvae of the genotype UAS-*cut*/+; *Gal4*[221], UAS-*mCD8::GFP*/+ and *Gal4*[221], UAS-*mCD8::GFP*/+ were covered in an amount of Halocarbon oil that restricted movement under a 50 × 22 coverslip but prevented bursting of the body wall. After imaging on a BioRad MRC 600 confocal microscope the slide was immersed in a dish of Halocarbon oil, the larva was recovered with forceps and left to develop until the next imaging session at 25°C on a grape juice agar plate with a small dollop of yeast paste.

References

Andres, V., Nadal-Ginard, B., and Mahdavi, V. (1992). Clox, a mammalian homeobox gene related to *Drosophila* cut, encodes DNA-binding regulatory proteins differentially expressed during development. Development *116*, 321–334.

Andres, V., Chiara, M.D., and Mahdavi, V. (1994). A new bipartite DNA-binding domain: cooperative interaction between the cut re-

peat and homeo domain of the cut homeoproteins. Genes Dev. 8, 245–257.

Arber, S., Ladle, D.R., Lin, J.H., Frank, E., and Jessell, T.M. (2000). ETS gene Er81 controls the formation of functional connections between group 1a sensory afferents and motor neurons. Cell 101, 485–498.

Beck, J.C., Murray, J.A., Willows, A.O., and Cooper, M.S. (2000). Computer-assisted visualizations of neural networks: expanding the field of view using seamless confocal montaging. J. Neurosci. Methods 98, 155–163.

Blochlinger, K., Bodmer, R., Jack, J.W., Jan, L.Y., and Jan, Y.N. (1988). Primary structure and expression of a product from cut, a locus involved in specifying sensory organ identity in Drosophila. Nature 333, 629–635.

Blochlinger, K., Bodmer, R., Jan, L.Y., and Jan, Y.N. (1990). Patterns of expression of Cut, a protein required for external sensory organ development in wild-type and cut mutant Drosophila embryos. Genes Dev. 4, 1322–1331.

Blochlinger, K., Jan, L.Y., and Jan, Y.N. (1991). Transformation of sensory organ identity by ectopic expression of Cut in Drosophila. Genes Dev. 5, 1124–1135.

Blochlinger, K., Jan, L.Y., and Jan, Y.N. (1993). Postembryonic patterns of expression of cut, a locus regulating sensory organ identity in Drosophila. Development 117, 441–450.

Bodmer, R., and Jan, Y.N. (1987). Morphological differentiation of the embryonic peripheral neurons in Drosophila. Roux's Arch. Dev. Biol. 196, 69–77.

Bodmer, R., Barbel, S., Sheperd, S., Jack, J.W., Jan, L.Y., and Jan, Y.N. (1987). Transformation of sensory organs by mutations of the cut locus of D. melanogaster. Cell 51, 293–307.

Bodmer, R., Carretto, R., and Jan, Y.N. (1989). Neurogenesis of the peripheral nervous system in Drosophila embryos: DNA replication patterns and cell lineages. Neuron 3, 21–32.

Brand, A.H., and Perrimon, N. (1993). Targeted gene expression as a means of altering cell fates and generating dominant phenotypes. Development 118, 401–415.

Brewster, R., and Bodmer, R. (1995). Origin and specification of type II sensory neurons in Drosophila. Development 121, 2923–2936.

Brewster, R., Hardiman, K., Deo, M., Khan, S., and Bodmer, R. (2001). The selector gene cut represses a neural cell fate that is specified independently of the Achaete-Scute Complex and atonal. Mech. Dev. 105, 57–68.

Briscoe, J., Pierani, A., Jessell, T.M., and Ericson, J. (2000). A homeodomain protein code specifies progenitor cell identity and neuronal fate in the ventral neural tube. Cell 101, 435–445.

Burz, D.S., Rivera-Pomar, R., Jackle, H., and Hanes, S.D. (1998). Cooperative DNA-binding by Bicoid provides a mechanism for threshold-dependent gene activation in the Drosophila embryo. EMBO J. 17, 5998–6009.

Dambly-Chaudière, C., and Ghysen, A. (1987). Independent subpatterns of sense organs require independent genes of the achaete-scute complex in Drosophila larvae. Genes Dev. 1, 297–306.

Driever, W., and Nüsslein-Volhard, C. (1988a). A gradient of bicoid protein in Drosophila embyros. Cell 54, 83–93.

Driever, W., and Nüsslein-Volhard, C. (1988b). The bicoid protein determines position in the Drosophila embryo in a concentration-dependent manner. Cell 54, 95–104.

Gao, F.B., Brenman, J.E., Jan, L.Y., and Jan, Y.N. (1999). Genes regulating dendrite outgrowth, branching, and routing in Drosophila. Genes Dev. 13, 2549–2561.

Grueber, W.B., Jan, L.Y., and Jan, Y.N. (2002). Tiling of the Drosophila epidermis by multidendritic sensory neurons. Development 129, 2867–2878.

Häusser, M., Spruston, N., and Stuart, G.J. (2000). Diversity and dynamics of dendritic signaling. Science 290, 739–744.

Huang, M.-L., Hsu, C.-H., and Chien, C.-T. (2000). The proneural gene amos promotes multiple dendritic neuron formation in the Drosophila peripheral nervous system. Neuron 25, 57–67.

Jack, J.W. (1985). Molecular organization of the cut locus of Drosophila melanogaster. Cell 42, 869–876.

Jan, Y.N., and Jan, L.Y. (2001). Dendrites. Genes Dev. 15, 2627–2641.

Jarman, A.P., Grau, Y., Jan, L.Y., and Jan, Y.N. (1993). atonal is a proneural gene that directs chordotonal organ formation in the Drosophila peripheral nervous system. Cell 73, 1307–1321.

Jessell, T.M. (2000). Neuronal specification in the spinal cord: inductive signals and transcriptional codes. Nat. Rev. Genet. 1, 20–29.

Kaminker, J.S., Canon, J., Salecker, I., and Banerjee, U. (2002). Control of photoreceptor axon target choice by transcriptional repression of Runt. Nat. Neurosci. 5, 746–750.

Koester, S.E., and O'Leary, D.D.M. (1992). Functional classes of cortical projection neurons develop dendritic distinctions by class-specific sculpting of an early common pattern. J. Neurosci. 12, 1382–1393.

Lee, T., and Luo, L. (1999). Mosaic analysis with a repressible cell marker for studies of gene function in neuronal morphogenesis. Neuron 22, 451–461.

Lee, T., Winter, C., Marticke, S.S., Lee, A., and Luo, L. (2000). Essential roles of Drosophila RhoA in the regulation of neuroblast proliferation and dendritic but not axonal morphogenesis. Neuron 25, 307–316.

Liu, S., McLeod, E., and Jack, J. (1991). Four distinct regulatory regions of the cut locus and their effect on cell type specification in Drosophila. Genetics 127, 151–159.

Livet, J., Sigrist, M., Stroebel, S., De Paola, V., Price, S.R., Henderson, C.E., Jessell, T.M., and Arber, S. (2002). ETS gene Pea3 controls the central position and terminal arborization of specific motor neuron pools. Neuron 35, 877–892.

Ludlow, C.R., Choy, R., and Blochlinger, K. (1996). Functional analysis of Drosophila and mammalian Cut protein in flies. Dev. Biol. 178, 149–159.

MacNeil, M.A., and Masland, R.H. (1998). Extreme diversity among amacrine cells: Implications for function. Neuron 20, 971–982.

Merritt, D.J. (1997). Transformation of external sensilla to chordotonal sensilla in the cut mutant of Drosophila assessed by single-cell marking in the embryo and larva. Microsc. Res. Tech. 39, 492–505.

Mollereau, B., Dominguez, M., Webel, R., Colley, N.J., Keung, B., de Celis, J.F., and Desplan, C. (2001). Two-step process for photoreceptor formation in Drosophila. Nature 412, 911–913.

Nepveu, A. (2001). Role of the multifunctional CDP/Cut/Cux homeodomain transcription factor in regulating differentiation, cell growth and development. Gene 270, 1–15.

Neufeld, E.J., Skalnik, D.G., Lievens, P.M., and Orkin, S.H. (1992). Human CCAAT displacement protein is homologous to the Drosophila homeoprotein, cut. Nat. Genet. 1, 50–55.

Quaggin, S.E., Vandenheuvel, G.B., Golden, K., Bodmer, R., and Igarashi, P. (1996). Primary structure, neural-specific expression, and chromosomal location of Cux-2, a second murine homeobox gene related to Drosophila cut. J. Biol. Chem. 271, 22624–22634.

Ramon y Cajal, S. (1911). Histology of the Nervous System of Man and Vertebrates. Paris.

Scott, E.K., and Luo, L. (2001). How do dendrites take their shape? Nat. Neurosci. 4, 359–365.

Struhl, G., Struhl, K., and Macdonald, P.M. (1989). The gradient morphogen bicoid is a concentration-dependent transcriptional activator. Cell 57, 1259–1273.

Threadgill, R., Bobb, K., and Ghosh, A. (1997). Regulation of dendritic growth and remodeling by Rho, Rac, and Cdc42. Neuron 19, 625–634.

Valarché, I., Tissier-Seta, J.P., Hirsch, M.R., Martinez, S., Goridis, C., and Brunet, J.F. (1993). The mouse homeodomain protein Phox2 regulates Ncam promoter activity in concert with Cux/CDP and is a putative determinant of neurotransmitter phenotype. Development 119, 881–896.

Vallstedt, A., Muhr, J., Pattyn, A., Pierani, A., Mendelsohn, M., Sander, M., Jessell, T.M., and Ericson, J. (2001). Different levels of

repressor activity assign redundant and specific roles to Nkx6 genes in motor neuron and interneuron specification. Neuron *31*, 743–755.

Vetter, P., Roth, A., and Häusser, M. (2001). Propagation of action potentials in dendrites depends on dendritic morphology. J. Neurophysiol. *85*, 926–937.

Wässle, H., and Boycott, B.B. (1991). Functional architecture of the mammalian retina. Physiol. Rev. *71*, 447–480.

Yoon, S.O., and Chikaraishi, D.M. (1994). Isolation of two E-box binding factors that interact with the rat tyrosine hydroxylase enhancer. J. Biol. Chem. *269*, 18453–18462.

Zipursky, S.L., Venkatesh, T.R., Teplow, D.B., and Benzer, S. (1984). Neuronal development in the *Drosophila* retina: monoclonal antibodies as molecular probes. Cell *36*, 15–26.